HHS Public Access

Author manuscript

Structure. Author manuscript; available in PMC 2016 May 05.

Published in final edited form as:

Structure. 2015 May 5; 23(5): 873–881. doi:10.1016/j.str.2015.02.014.

Tubulation by amphiphysin requires concentration-dependent switching from wedging to scaffolding

J. Mario Isas[1,*], **Mark R. Ambroso**[1,*], **Prabhavati B. Hegde**[1], **Jennifer Langen**[2], and **Ralf Langen**[1,¥]

[1]Zilkha Neurogenetic Institute, University of Southern California, Los Angeles, California 90033, USA

[2]Department of Biological Sciences, University of Southern California, Los Angeles, CA 90089-2910, USA

Summary

BAR proteins are involved in a variety of membrane remodeling events, but how they can mold membranes into different shapes remains poorly understood. Using EPR, we find that vesicle binding of the N-BAR protein amphiphysin is predominantly mediated by the shallow insertion of amphipathic N-terminal helices. In contrast, the interaction with tubes involves deeply inserted N-terminal helices together with the concave surface of the BAR domain, which acts as a scaffold. Combined with the observed concentration dependence of tubulation and BAR domain scaffolding, the data indicate that initial membrane deformations and vesicle binding are mediated by insertion of amphipathic helical wedges, while tubulation requires high protein densities at which oligomeric BAR domain scaffolds form. In addition, we identify a pocket of residues on the concave surface of the BAR domain that deeply insert into tube membrane. Interestingly, this pocket harbors a number of disease mutants in the homologous amphiphysin 2.

Introduction

The remodeling of cellular membranes is controlled by proteins that sense, stabilize or induce membrane curvature (Rao and Haucke, 2011; Zimmerberg et al., 2006). Examples of membrane remodeling include vesicle budding and fusion events as well as the formation of cylindrical tubes in the cell. BAR domain-containing proteins have recently risen to prominence as they are involved in a wide range of membrane remodeling events. Amphiphysin is an N-BAR protein involved in endocytosis as well as T-tubule formation (Butler et al., 1997; David et al., 1994; De Camilli et al., 1993; Kukulski et al., 2012; Lee et al., 2002; Meinecke et al., 2013; Razzaq et al., 2001). The deletion of amphiphysin in

¥Corresponding Author: Ralf Langen, Zilkha Neurogenetic Institute, 1501 San Pablo St., 121 ZNI, Los Angeles, CA 90033. Tel.: 323-442-1323 Fax: 323-442-4404. langen@usc.edu.

*J.M.I. and M.R.A. contributed equally to this work.

Drosophila destabilizes the T-tubule network and mutations in humans have been shown to cause muscle diseases including centronuclear myopathy (Böhm et al., 2014; Claeys et al., 2010; Nicot et al., 2007; Razzaq et al., 2001). Endocytosis as well as T-tubule formation involves the shaping of membranes into curved entities, but while T-tubule formation results in the generation of elongated tubular structures, endocytosis is a more dynamic process that leads to the formation of curved vesicles. The ability of N-BAR proteins to partake in the formation or stabilization of different types of membrane curvature is also seen *in vitro*. Amphiphysin and the related N-BAR protein endophilin are capable of forming bilayer tubes of different diameter as well as cylindrical micelles and small highly curved vesicles (Farsad et al., 2001; Mizuno et al., 2010; Mim et al., 2012; Peter et al., 2004). Two of the main mechanisms that have been discussed for the formation of such structures are scaffolding and the wedging of amphipathic helices.

The first evidence that amphiphysin and endophilin might be able to promote membrane curvature via scaffolding came from structural studies which showed that these proteins are banana-shaped dimers (Gallop et al., 2006; Peter et al., 2004; Weissenhorn, 2005). As shown with the example of amphiphysin (Figure 1A), these dimers have a curvature complementary to that of the tubes they form. Moreover, the dimers are known to further associate into larger oligomeric networks on tubes (Mim et al., 2012; Mizuno et al., 2010; Takei et al., 1999; Yin et al., 2009). It has, therefore, been proposed that these proteins act via a scaffolding mechanism in which rigid BAR domain oligomers impose their shape onto the membrane and promote positive curvature. The concept of using scaffolding for controlling membrane curvature has since been expanded to other types of BAR domain proteins, such as F-BAR and I-BAR proteins (Arkhipov et al., 2009; Frost et al., 2008; Henne et al., 2007; Itoh et al., 2005; Pykäläinen et al., 2011; Saarikangas et al., 2009; Shimada et al., 2007; Yu and Schulten, 2013). However, membrane curvature induction by amphiphysin and endophilin does not solely rely on their BAR domains as other regions outside of the BAR domain are critical for tubulation as well. For example, mutations in the N-terminal regions of amphiphysin and endophilin as well as mutations in an insert region that is present in endophilin but not in amphiphysin, have been shown to significantly inhibit tubulation (Farsad et al., 2001; Gallop et al., 2006; Itoh and De Camilli, 2006; Peter et al., 2004). Site directed spin labeling (SDSL) studies using electron paramagnetic resonance (EPR) (Gallop et al., 2006; Jao et al., 2010) as well as computational studies (Blood and Voth, 2006; Blood et al., 2008; Cui et al., 2009, 2013; Mim et al., 2012) were able to verify that all of these regions fold up into amphipathic helical structures that are thought to act as wedges in the membrane. Work on the Parkinson's disease protein α-synuclein has shown that helical wedges can be sufficient for inducing tubulation, demonstrating that scaffolding is not a prerequisite for membrane bending (Varkey et al., 2010; Westphal and Chandra, 2013). Interestingly, endophilin's BAR domain was found to be at a significant distance away from the membrane under vesiculating conditions suggesting that the amphipathic helices might be the predominant curvature-stabilizing entities (Jao et al., 2010). In order to address the apparent discrepancy with respect to the importance of scaffolding and helix insertion, a recent study used using SDSL and EPR found that endophilin employs different structures and mechanisms to generate vesicles or tubes (Ambroso et al., 2014). The central finding was that the N-terminal and insert region helices were more deeply embedded in

tube than vesicle membranes. Based on membrane proximity measurements of two residues, it was also suggested that this helical movement is coupled to a shift of the BAR domain towards the membrane. This movement could significantly enhance the scaffolding activity of the BAR domain. However, the precise orientations of endophilin's BAR domain with respect to vesicle or tube membranes remain unknown. Moreover, a recent study on the BAR protein ACAP1 suggested that tube formation is not directly mediated by the BAR domain but by membrane interaction with its pleckstrin homology domain (Pang et al., 2014). Thus, tube formation may not require BAR domain-dependent scaffolding. Amphiphysin is different from endophilin and ACAP1 as it lacks insert helices or PH domains. We therefore set out to test (a) whether the BAR domain of amphiphysin is involved in scaffolding and (b) whether amphiphysin uses different mechanisms to interact with vesicles or tubes. In order to obtain detailed structural information for the membrane interaction of the BAR domain and N-terminal helix of amphiphysin (henceforth referred to as amphiphysin), we performed SDSL for 49 spin labeled sites in the BAR domain and 14 sites in the N-terminus. We then used EPR of these spin labeled derivatives to investigate the structures of amphiphysin bound to vesicles or tubes. In support of a scaffolding mechanism, we find that the entire concave surface of the BAR domain comes into direct contact with the tube membrane. Residues on this surface exhibit significant membrane interaction with all sites at least penetrating into the lipid headgroup region. The most deeply inserted residues (144, 147, and 151) were found in a pocket that even inserts into the acyl chain region of the membrane. Interestingly, both this pocket and the N-terminal helix, which we find to differentially interact with tubes and vesicles, are in the immediate vicinity of known familial disease mutants (Böhm et al., 2014; Claeys et al., 2010; Nicot et al., 2007; Razzaq et al., 2001). In contrast to tubes, scaffolding does not seem to be important on vesicles where the BAR domain only minimally contacts the membrane and where membrane interaction is predominantly mediated by the N-terminal helices.

Results

Amphiphysin vesicle binding is mediated by shallow insertion of its amphipathic N-terminal helix

In order to compare the structures of vesicle and tube bound amphiphysin, we sought conditions that resulted in clean preparations of amphiphysin either bound to vesicles or tubes. We found that amphiphysin both vesiculated and tubulated vesicles containing the commonly used total brain lipids. While it was possible to enrich for vesicles and tubes, it was difficult to obtain clean preparations containing only tubes or vesicles. This problem was further compounded by significant batch-to-batch variations in the total brain lipid extracts. Thus, we examined a large number of conditions and found two different defined lipid compositions that resulted in amphiphysin stably bound to either vesicles or tubes. The structure of amphiphysin bound to the respective structures was then studied using SDSL and EPR spectroscopy. Toward this end, we introduced spin labels, one amino acid at a time, at 14 selected sites in the N-terminal region of amphiphysin (not resolved in the crystal structure) and 49 sites throughout the BAR domain (Figure 1A). First, we examined the changes in structure and membrane topography that occur as amphiphysin binds to vesicles containing a mixture of phosphatidylserine and cholesterol (Figure 1B). The EPR spectra for

N-terminally labeled sites revealed that this region is unfolded in solution (Figure S1A) explaining why the N-terminus was not resolved in the crystal structure. The change in the EPR spectra upon vesicle binding, however, reveals reduced mobility and ordering of the N-terminus (Figure S1B). In order to determine the orientation of the N-terminus with respect to the vesicle membrane, we measured the membrane immersion depths of each spin labeled site through accessibility measurements (Figure S1C and S1D). These measurements take advantage of the well established collision gradients that increase toward the center of the membrane in the case of hydrophobic O_2, while the opposite is observed for collisions with hydrophilic NiEDDA (Altenbach et al., 1994). The data can be conveniently summarized with the depth parameter Φ, which is defined by $\Phi=\ln(\Pi O_2/\Pi NiEDDA)$. Larger Φ values indicate increasing membrane immersion depths (Altenbach et al., 1994; Frazier et al., 2003). As illustrated in Figure 1C, Φ oscillates as a function of N-terminal sequence with a periodicity that indicates that the N-terminus folds into an α-helix upon membrane binding Hubbell et al., 1998). When plotted onto a helical wheel (Figure 1D), all lipid exposed residues local maxima in Φ plot, *red*) are on one face, while all solvent exposed residues (local minima in Φ plot, *blue*) are on the other, suggesting the helix is amphipathic. Based upon calibration using spin labeled lipids (*see methods*, Figure S1E), we find that the deepest lipid exposed sites are located at immersion depths of 7 to 10 Å. Considering the extension of the R1 side chain (~7 to 10 Å from the center of an α-helix) (Langen et al., 2000), the N-terminal helix is parallel to the membrane with its center approximately at the level of the head group phosphates, where it is well positioned to act as a molecular wedge (Figure 1E) (Campelo et al., 2008, 2010; Drin and Antonny, 2010).

Next we investigated the structure and membrane proximity of the BAR domain on vesicles. Comparison of the EPR spectra for spin labeled derivatives bound to vesicles or in solution revealed that mobility changes between the two states were highly localized (Figure S1F and S1G). These changes are summarized in Figure 1F using the central line width, a commonly employed mobility parameter (Jao et al., 2004). Little or no mobility changes were observed at sites near the convex side of the protein as well as at the more central regions along the concave surface of the BAR domain. In contrast, the strongest immobilization was observed near the tip region of amphiphysin for residues 146, 148, 150–153, 168, 170–174, and 176. These residues are located at the end of helix 2 and the beginning of helix 3, respectively (Figure 1A and 1H). In solution, these regions have multi-component EPR spectra indicative of ordered and disordered structure consistent with frayed helical ends. Upon vesicle binding these regions become much more ordered. The high mobility in the intervening loop region (residues 156 to 167) remains. When accessibility measurements were performed, no labeling site in the BAR domain gave rise to strongly enhanced O_2 accessibilities (Figure 1G; Table S1). Φ values for all sites ranged between −0.9 and −2, values that are typically observed for soluble proteins in aqueous solution under these conditions (Shah et al., 2014). Importantly, all sites lie outside the region for which immersion depth is calibrated, from the interior of the bilayer to ~5 Å above the phosphate level (Figure 1G, *dashed line*; Figure S1E). This lack of calibration precludes us from directly determining the precise location of the BAR domain relative to the membrane, however the data still allow us to estimate a lower limit for the distance between the BAR domain and the vesicle membrane. Considering that all sites lay outside the calibrated depth range, their nitroxide moieties must

be at least 5 Å above the phosphate level. Many labeled sites include residues on the concave surface of the BAR domain and are predicted to project directly toward the membrane. Since the backbone is at least another 7 Å away from the nitroxide moiety, we can therefore estimate that the backbone to phosphate distance in these cases must be at least 12 Å. Thus, if the BAR domain contacts the membrane, such contacts must be limited to interactions with the more distal region of the headgroups. Considering the different geometries of the modestly curved membrane and the highly curved BAR domain, such contacts could involve the tip region of the BAR domain (Figure 1H), which experiences a significant reduction in mobility upon vesicle binding. However, we cannot exclude the possibility that vesicle interaction causes an ordering of the frayed helical ends via alternative mechanisms that do not require physical contact of this region with the membrane.

On tubes, the BAR domain comes into contact with the membrane and N-termini move deeper into the bilayer

In order to compare the structure of vesicle bound amphiphysin with that of the tube bound protein, we repeated the experiments under tubulating conditions using phosphatidylglycerol and phosphatidylethanolamine containing vesicles. Under the conditions used, the membranes became completely tubulated with a well defined, highly oligomeric protein coat (Figure 2A and 2B). The EPR spectra of sites in the N-terminal region revealed that this region also becomes ordered on tubes (Figure S2A and S2B). Moreover, the periodicity in the accessibility data (Figures 2C and S2C) again indicated the formation of α-helical structure. When compared to the vesicle bound form, however, much larger Φ values were obtained for the N-terminus on tubes indicating deeper membrane insertion. According to the calibration (Figure S2D), the most deeply inserted residues are on average ~16 Å below the phosphate level. Taking into account the 7–10 Å length of the spin labeled moiety from the center of the α-helix (Langen et al., 2000), we approximate the helical wedges to be driven more deeply into the tube membrane with their centers penetrating about 6–9 Å into the acyl chain region (Figure 2D).

Having established that the location of the N-terminal helices differs between vesicles and tubes, we next wanted to determine whether similar changes might also occur in the BAR domain. As in the case of vesicle binding, tubulation caused spectral changes for spin labeled sites in the BAR domain that were highly dependent on where the label was introduced (Figure S3A and S3B). Again, the EPR spectral changes were mainly limited to sites located on the concave surface. However, there were also some distinctive differences between the spectra of the vesicle and tube bound proteins. A comparison of the central line widths revealed that the mobility of the vesicle and tube bound states differed most for sites on the concave surface (Figure S3C and S3D). The most pronounced differences were observed for residues 58, 97, 113, 133, 151, 154, 158 and 171, most of which are spread out over the presumed membrane interaction surface. This is in contrast to the more localized mobility changes observed mainly in the tip region for the vesicle bound protein. To test whether this enhanced ordering of residues on the concave surface is accompanied by altered membrane proximity of the BAR domain, we again performed O_2 and NiEDDA accessibility measurements. The respective accessibilities are given in Table S1 and are

summarized by the Φ values in Figure 3A. As in the case of vesicle bound amphiphysin, sites on the convex surface again resulted in negative Φ values indicating that these regions do not come into direct contact with the membrane. However when labeling occurred at the concave surface, more positive Φ values could be seen indicating membrane proximity or membrane penetration for those sites. The largest Φ values were obtained for residues 58, 133, 144, 147, 148, 151, 154, 170, and 171 indicating that residues on the concave surface of the BAR not only become more ordered but that they also come into closer proximity to the membrane. These enhanced Φ values are not the consequence of a previously observed steric exclusion of NiEDDA (Isas et al., 2002) but are instead due to enhanced accessibility to O_2 (Figure S3E). While the accessibility values for most of these sites are consistent with a location near the lipid headgroup level, a cluster of residues (144, 147, and 151) penetrates more deeply (nitroxide moiety at 2–7 Å immersion depth) into the acyl chain region (Figures 3B and S2D).

Tubulation and BAR domain scaffolding are dependent on protein concentration

Recent studies using mechanically pulled nanotubes found two distinct ways in which amphiphysin or endophilin can stabilize membrane curvature (Sorre et al., 2012; Zhu et al., 2012). At dilute protein conditions, the effect of these proteins was relatively modest, but at higher protein-to-lipid ratios they became more potent and stabilized tubes similar in size to those generated here. In order to test how different protein concentrations might affect amphiphysin membrane interaction, we repeated the tubulation experiments at four fold lower protein-to-lipid ratios. According to negative stain electron microscopy, these conditions reduced overall tubulation and more vesicular structures were present (Figure 3C). As expected from the more abundant presence of vesicles, accessibility measurements resulted in a significant reduction of Φ values indicating reduced interaction of the BAR domain with the membrane (Figure 3D). These experiments suggest that a threshold protein-to-lipid ratio is required in order for stable tubulation to occur. Inasmuch as tubulation coincides with the formation of an oligomeric protein coat around the tubes, it is likely that the switch to scaffolding is coupled to oligomer formation.

The finding that decreasing protein-to-lipid ratios cause reduced tubulation as well as reduced Φ values also served as an important control. Our analysis of tube and vesicle-bound protein in Figures 1, 2, 3A and 3B used two different lipid compositions, while the data in Figure 3C and 3D used the same lipid composition. Thus, the strong effects on the Φ values in Figure 3D must be due to the decreased yield of tubulation and not lipid composition. To further address this issue, we also investigated the Φ values from selected amphiphysin derivatives bound to total brain lipid membranes. Again we observed the same trend that preparations enriched for tubes had more positive Φ values than those enriched for vesicles (data not shown).

Discussion

In this study, we set out (a) to determine what mechanisms amphiphysin uses to bend lipid membranes and (b) to provide a detailed structural analysis of the BAR domain on tubes and vesicles. Our structural analysis revealed that amphiphysin uses different structures and

mechanisms to interact with vesicle or tube membranes. The BAR domain only weakly contacts the vesicle membrane. Vesicle interaction reduces the mobility at the tip regions of the BAR domain but even these residues do not experience significant membrane immersion. Thus, if there is any interaction between the BAR domain and the membrane, it is likely limited to contacts with the more distal portions of the lipid head groups. In contrast, tube binding involves the entire concave surface of the BAR domain. Residues throughout this surface are in direct contact with the membrane and penetrate deeply into the headgroup region and in some cases even into the acyl chain region. This downward movement allows the BAR domain to impart its own curved structure onto the membrane and act as a scaffold. Scaffolding is further aided by the formation of specific oligomeric structures that wrap around the tubes (Figure 2B) (Mim et al., 2012; Mizuno et al., 2010; Takei et al., 1999). We also find that the N-terminus is capable of forming three distinct structures: (a) a random coil in solution, (b) an amphipathic helix shallowly inserted into vesicles, or (c) an amphipathic helix deeply inserted into the tube membrane.

The movement of the BAR domain toward the tube membrane allows for numerous positively charged residues on its concave surface to engage in electrostatic interactions with negative charges on the lipid headgroups. This interaction is likely to contribute a significant amount of energy towards the formation of a tight scaffold. Although the entire concave surface is in contact, the binding interactions are not perfectly uniform. Interestingly, we identified a pocket of amino acids (~144 to 151) with reduced mobility that more deeply penetrate into the tube membrane than other amino acids on the concave surface of the BAR domain (Figure 3A and 3B). The importance of this region is further illustrated by the fact that the homologous region in amphiphysin 2 harbors mutations found in familial forms of centronuclear myopathy (Claeys et al., 2010; Nicot et al., 2007). These D151N and R154Q mutations (corresponding to position D146 and R149 in the present study) are thought to inhibit tubulation *in vivo* as well as *in vitro* (Claeys et al., 2010; Nicot et al., 2007; Wu et al., 2014). One possibility is that this membrane insertion pocket makes specific lipid contacts. In fact, a recent study on F-BAR proteins identified a conserved lipid binding site on the concave membrane binding surface of these proteins (Moravcevic et al., 2015). A specific coordination of lipids is consistent with the strong immobilization observed in the EPR spectra for this region, as prior studies on annexins have shown that specific lipid coordination results in pronounced immobilization (Isas et al., 2002). In principle, protein-protein contacts, such as contacts with N-terminal helices, could contribute to the observed immobilization as well. For example, one could envisage an interaction between N-terminal helices from one dimer with a BAR domain from an adjacent dimer. Such an interaction could stabilize the oligomeric coats on tubes and couple the movement of the BAR domain to the movement of the N-terminal helices. However, such contacts were not resolved in cryoEM reconstructions of endophilin tubes (Mim et al., 2012; Mizuno et al., 2010) and additional studies will be needed to test for this possibility. Regardless of the precise mechanism, geometric considerations may explain why oligomerization is more pronounced on tubes. While a vesicle is isotropically curved (curved in 3 dimensions), a tube is curved anisotropically with curvature around but not along its axis. We would therefore expect vesicle-associated BAR proteins to follow the isotropic curvature of the vesicle and to be oriented in various directions. In contrast, tube-bound BAR proteins are much more likely to

be aligned in similar orientations in order to stabilize the anisotropic curvature. Oligomerization should greatly facilitate such an alignment.

The finding that amphiphysin's N-terminal helices are the primary membrane interacting region on vesicles is consistent with a recent microscopy study that found the BAR domain alone to possess little curvature sensitivity toward vesicles; rather membrane curvature sensing was mainly mediated by the N-terminal helices (Bhatia et al., 2009). The shallow insertion of amphiphysin's N-terminal helices is a common conformation also observed for vesicle binding of amphipathic helices from epsin, α-synuclein and endophilin (Gallop et al., 2006; Jao et al., 2008, 2010; Lai et al., 2012). A computational study indicated that shallowly inserted helices selectively wedge into the head groups (Campelo et al., 2010), thereby stabilizing curvature in a manner akin to the spontaneous curvature effect of lipids with large headgroups and small acyl chains. On tubes, however, the N-terminal helices submerge beyond the lipid phosphates and into the acyl chain region where they produce a reduced amount of spontaneous curvature (Campelo et al., 2008, 2010). In addition to no longer applying pressure exclusively to the headgroup region, the N-terminal helices may also push the acyl chain regions apart. This feature may be beneficial for tubulation by allowing amphiphysin to compensate for lipid vacancies that occur as a target vesicle is being remodeled into a tubular structure, where the surface area of the outer leaflet increases significantly, requiring additional lipids or protein to fill out the leaflet. The ability to take up space in the outer leaflet may be particularly important in cases where lipid flip-flop is slow or inefficient such as in the case of membranes with low cholesterol content. The deep insertion of the amphipathic helices may also alter the structural organization of nearby lipids. The interaction of the amphipathic helices with adjacent lipids is likely to cause a bending of these lipids, which in turn will cause local membrane thinning. This bending could occur for two reasons, 1) the negatively charged moieties of the lipid headgroups are expected to bend around the hydrophilic surface of the amphipathic helices to interact with positively charged residues (Ambroso et al., 2014), and 2) the acyl chains are likely to bend around the hydrophobic surface of the helices to take up otherwise empty space between the helices and the center of the bilayer. Inasmuch as membrane thickness is inversely related to rigidity, local membrane thinning would facilitate membrane bending. Moreover, the thinning of the membrane could make protein oligomerization energetically favorable. Close spatial proximity of two helical wedges brings two locally thinned membranes together, limiting the number of energetically unfavorable membrane thickness transitions. Such matching of membrane thickness has previously been found to be an important factor in clustering transmembrane proteins (Haselwandter and Phillips, 2013; Haselwandter and Wingreen, 2014).

It should be noted that disease mutations found in centronuclear myopathy are not limited to the BAR domain of amphiphysin 2 as several mutants have been mapped to the N-terminus (K21del and R24C; K16 and R19 respectively for the structurally homologous amphiphysin used in this study) (Böhm et al., 2014; Claeys et al., 2010; Nicot et al., 2007). The interesting similarity between the mutations in the BAR domain and the N-terminus is that they all become more deeply inserted in the tube bound state. How the mutations affect these conformational transitions remains to be tested.

A prior study found that increased length or number of helical wedges promoted vesiculation while enhanced scaffolding promoted tubulation (Boucrot et al., 2012). Our finding that vesiculation is mainly mediated by the insertion of amphipathic helices while tubulation is accompanied by enhanced scaffolding is in good agreement with this notion. However, our data also reveal an important detail, namely that the overall length and number of helices is not the only consideration. This is because the same protein has the ability to switch between different structural states that either rely on wedging or a combination of wedging and scaffolding. A dichotomy of mechanisms used by amphiphysin to interact with membranes is further consistent with previous work in which amphiphysin was found to mainly sense curvature in conditions of low protein density while inducing curvature at higher protein densities (Sorre et al., 2012). Our structural data indicate that the enhanced ability to cause extensive tubulation at higher protein densities is caused by movements of the BAR domain and the amphipathic helices toward the membrane that occur as the oligomeric scaffolds are formed. Taking all of these data together, it appears likely that the initial membrane interactions of amphiphysin at low protein densities are predominately mediated by the wedging of amphipathic helices (Figure 4A). Such wedging could then create an initial membrane bending. As the membrane bending increases and amphiphysin reaches a threshold density, the BAR domains undergo a concerted structural reorganization that brings them closer to the membrane, allows them to form an oligomeric scaffold, and lets their N-terminal helices insert more deeply into the membrane (Figure 4B). Our study is consistent with previous studies (Boucrot et al., 2012; Sorre et al., 2012) which indicate that a minimum threshold of amphiphysin density is required for extensive tubulation. That does not mean that continuously raising the protein density will only generate more tubes. In fact, Boucrot et al. find vesiculation to occur at very high protein densities of BAR proteins, and we made similar observations for α-synuclein-dependent membrane remodeling (Varkey et al., 2010, 2013).

The different structures and mechanisms used to bind tubes and vesicles may also have implications for the regulation of membrane curvature *in vivo*. By preferentially stabilizing the vesicle or tube bound form of the protein it may be possible to guide membrane remodeling *in vivo*. Recent studies suggests that phosphorylation of endophilin at position S75 favors the vesicle bound form of this protein (Ambroso et al., 2014), and is a regulatory mechanism in synaptic endocytosis (Matta et al., 2012). Thus, the use of post-translational modifications may be an effective means for controlling different types of membrane curvature. Interestingly, amphiphysin has also been found to contain a phosphorylation site in its N-terminus (Hornbeck et al., 2012). Future studies will have to show whether post-translational modifications are used to regulate which types of membrane curvature amphiphysin generates *in vivo*.

Experimental Procedures

Generation of amphiphysin mutants and spin labeled derivatives

The plasmid containing His_6-tagged N-BAR domain (a.a. 1–244) of Drosophila Amphiphysin (Peter et al., 2004) was kindly provided by Dr. Harvey McMahon (Medical Research Council). In order to allow specific labeling of cysteine residues, C66 and C82

were mutated to alanine by site-directed mutagenesis (QuikChange, Stratagene). Single cysteine mutants were then introduced and verified by sequencing. Proteins were expressed as previously described (Varkey et al., 2010) in *E. coli* BL21 (DE3) and purified using nickel-nitrilo-triacetic acid–agarose, followed by superdex 200 gel filtration. Remaining impurities were removed using mono S cation exchange chromatography with a low salt buffer A (20 mM hepes pH 7.4, 1 mM dithiothreitol (DTT)) and elution buffer B (20 mM hepes pH 7.4, 2 M NaCl and 1 mM DTT). Protein concentrations were determined by absorbance at 280 nm using an extinction coefficient $\varepsilon = 21860\ M^{-1}cm^{-1}$.

Immediately prior to spin labeling, DTT was removed via size exclusion (PD-10 (GE)) columns equilibrated in 20 mM hepes, pH 7.4, 500 mM NaCl. Spin label (1-oxyl-2,2,5,5 tetramethyl-Δ3-pyrroline-3-methylmethanethiosulfonate) was incubated with protein in a 3 to 5 fold molar excess at room temperature for one hour, or alternatively, at 4° C overnight. Unreacted spin label was removed using PD-10 columns as described above.

Vesicle preparation and amphiphysin membrane interaction

The following synthetic lipids were used: 1-palmitoyl-2-oleoyl-*sn*-glycero-3-phosphoethanolamine (POPE), 1-palmitoyl-2-oleoyl-*sn*-glycero-3-phospho-L serine (POPS), 1-palmitoyl-2-oleoyl-*sn*-glycero-3-[phospho-RAC-(1-glycerol)] (POPG), and cholesterol (Avanti Polar Lipids, Alabaster, AL). For tubulation experiments, large multi-lamellar vesicles were prepared by vortexing the dried lipid film containing POPG/POPE (2:1, weight:weight) in buffer A. The various labeled and unlabeled forms of amphiphysin were incubated with vesicles at a protein-to-lipid ratio of 1:10 weight:weight) wherein the protein was added last. In each case, tubulation was verified using negative-stain transmission electron microscopy. For vesicle binding small, extruded vesicles containing POPS and cholesterol were made by mixing POPS/Cholesterol (4:1, weight:weight) and vortexing the dried lipid in 20 mM hepes, pH 7.4, 150 mM NaCl. The vesicles were then treated to 10 cycles of freezing and thawing and then extruded using a mini-extruder with a 100 nm cutoff polycarbonate membrane (Avanti Polar Lipids, Alabaster, AL). For vesicle binding, protein and lipid were mixed at a 1:10 weight to weight ratio and incubated at room temperature for 20 minutes. Again, electron microscopy was used to assay sample homogeneity. Under these conditions, vesicles stayed intact and did not show any significant change in size.

Acquisition and analysis of EPR data

Continuous wave EPR spectra were recorded using a Bruker EMX spectrophotometer fitted either with an ER4119HS resonator or a Bruker dielectric resonator. The latter was also used for all power saturation experiments. The scan width for all EPR spectra is 100 Gauss. For EPR experiments, tube bound amphiphysin was harvested by centrifugation at 16,000 g in a micro centrifuge and vesicle bound amphiphysin at 120,000 g in an ultra centrifuge (Beckman Coulter Inc., Brea, CA). Pellets were taken up in Quartz capillaries VitroComInc., New Jersey) for recording continuous wave EPR spectra and in TPX capillaries for accessibility measurements. Accessibilities to O_2 and NiEDDA (ΠO_2 and ΠNiEDDA) were measured by power saturation at room temperature (Altenbach et al., 1994). O_2 measurements were performed with samples equilibrated with air and NiEDDA

measurements were performed using exogenously added NiEDDA to a final concentration of 10 mM. The membrane immersion depth for lipid-exposed residues was calculated from the depth parameter Φ (Altenbach et al., 1994). Φ was calibrated for depth by doping the lipid mixtures mentioned above with 1% of 1-palmitoyl-2-DOXYL-stearoyls*n*-glycero-3-phosphocholine (Avanti PolarLipids, Alabaster, AL) spin-labeled at positions 5, 7, 10 and 12 on the acyl chains as well as the tempo labeled (1-palmitoyl-2-oleoyl-*sn*-glycero-3-phospho(tempo)choline) derivative containing a spin label in the headgroup region (Figure S1E and S2D).

Electron microscopy

Small aliquots (~10 μL) of tube or vesicle bound amphiphysin sample were incubated with carbon-coated formvar films mounted on copper grids (Electron Microscopy Services, Hatfield) for 5 minutes. Excess liquid was removed using filter paper and the grids were immediately stained with 1% uranyl acetate for 1 minute, rinsed thrice with 10 μL additional 1% uranyl acetate, and subsequently dried. A JEOL 1400 transmission electron microscope was used for specimen observation at 100 kV.

Supplementary Material

Refer to Web version on PubMed Central for supplementary material.

Acknowledgements

This work was supported by National Institutes of Health Grants GM063915 (to R.L.). Author Contributions: J.M.I., M.R.A, P.H., J.L. performed research. R.L. and M.R.A. wrote the paper.

Manuscript References

Altenbach C, Greenhalgh DA, Khorana HG, Hubbell WL. A collision gradient method to determine the immersion depth of nitroxides in lipid bilayers: application to spin-labeled mutants of bacteriorhodopsin. Proc. Natl. Acad. Sci. U. S. A. 1994; 91:1667–1671. [PubMed: 8127863]

Ambroso MR, Hegde BG, Langen R. Endophilin A1 induces different membrane shapes using a conformational switch that is regulated by phosphorylation. Proc. Natl. Acad. Sci. 2014; 111:6982–6987. [PubMed: 24778241]

Bhatia VK, Madsen KL, Bolinger P-Y, Kunding A, Hedegård P, Gether U, Stamou D. Amphipathic motifs in BAR domains are essential for membrane curvature sensing. EMBO J. 2009; 28:3303–3314. [PubMed: 19816406]

Blood PD, Voth GA. Direct observation of Bin/amphiphysin/Rvs (BAR) domain-induced membrane curvature by means of molecular dynamics simulations. Proc. Natl. Acad. Sci. U. S. A. 2006; 103:15068–15072. [PubMed: 17008407]

Blood PD, Swenson RD, Voth GA. Factors influencing local membrane curvature induction by N-BAR domains as revealed by molecular dynamics simulations. Biophys. J. 2008; 95:1866–1876. [PubMed: 18469070]

Böhm J, Biancalana V, Malfatti E, Dondaine N, Koch C, Vasli N, Kress W, Strittmatter M, Taratuto AL, Gonorazky H, et al. Adult-onset autosomal dominant centronuclear myopathy due to BIN1 mutations. Brain. J. Neurol. 2014

Boucrot E, Pick A, Çamdere G, Liska N, Evergren E, McMahon HT, Kozlov MM. Membrane fission is promoted by insertion of amphipathic helices and is restricted by crescent BAR domains. Cell. 2012; 149:124–136. [PubMed: 22464325]

Butler MH, David C, Ochoa GC, Freyberg Z, Daniell L, Grabs D, Cremona O, De Camilli P. Amphiphysin II (SH3P9; BIN1), a member of the amphiphysin/Rvs family, is concentrated in the cortical cytomatrix of axon initial segments and nodes of ranvier in brain and around T tubules in skeletal muscle. J. Cell Biol. 1997; 137:1355–1367. [PubMed: 9182667]

Campelo F, McMahon HT, Kozlov MM. The hydrophobic insertion mechanism of membrane curvature generation by proteins. Biophys. J. 2008; 95:2325–2339. [PubMed: 18515373]

Campelo F, Fabrikant G, McMahon HT, Kozlov MM. Modeling membrane shaping by proteins: focus on EHD2 and N-BAR domains. FEBS Lett. 2010; 584:1830–1839. [PubMed: 19836393]

Claeys KG, Maisonobe T, Böhm J, Laporte J, Hezode M, Romero NB, Brochier G, Bitoun M, Carlier RY, Stojkovic T. Phenotype of a Patient with Recessive Centronuclear Myopathy and a Novel Bin1 Mutation. Neurology. 2010; 74:519–521. [PubMed: 20142620]

Cui H, Ayton GS, Voth GA. Membrane binding by the endophilin N-BAR domain. Biophys. J. 2009; 97:2746–2753. [PubMed: 19917228]

Cui H, Mim C, Vázquez FX, Lyman E, Unger VM, Voth GA. Understanding the role of amphipathic helices in N-BAR domain driven membrane remodeling. Biophys. J. 2013; 104:404–411. [PubMed: 23442862]

Drin G, Antonny B. Amphipathic helices and membrane curvature. FEBS Lett. 2010; 584:1840–1847. [PubMed: 19837069]

Farsad K, Ringstad N, Takei K, Floyd SR, Rose K, De Camilli P. Generation of high curvature membranes mediated by direct endophilin bilayer interactions. J. Cell Biol. 2001; 155:193–200. [PubMed: 11604418]

Frazier AA, Roller CR, Havelka JJ, Hinderliter A, Cafiso DS. Membrane-Bound Orientation and Position of the Synaptotagmin I C2A Domain by Site-Directed Spin Labeling†. Biochemistry (Mosc.). 2003; 42:96–105.

Frost A, Perera R, Roux A, Spasov K, Destaing O, Egelman EH, De Camilli P, Unger VM. Structural basis of membrane invagination by F-BAR domains. Cell. 2008; 132:807–817. [PubMed: 18329367]

Gallop JL, Jao CC, Kent HM, Butler PJG, Evans PR, Langen R, McMahon HT. Mechanism of endophilin N-BAR domain-mediated membrane curvature. EMBO J. 2006; 25:2898–2910. [PubMed: 16763559]

Haselwandter CA, Phillips R. Connection between Oligomeric State and Gating Characteristics of Mechanosensitive Ion Channels. PLoS Comput Biol. 2013; 9:e1003055. [PubMed: 23696720]

Haselwandter CA, Wingreen NS. The role of membrane-mediated interactions in the assembly and architecture of chemoreceptor lattices. PLoS Comput. Biol. 2014; 10:e1003932. [PubMed: 25503274]

Henne WM, Kent HM, Ford MGJ, Hegde BG, Daumke O, Butler PJG, Mittal R, Langen R, Evans PR, McMahon HT. Structure and analysis of FCHo2 F-BAR domain: a dimerizing and membrane recruitment module that effects membrane curvature. Struct. Lond. Engl. 2007; 15:839–852. 1993.

Hornbeck PV, Kornhauser JM, Tkachev S, Zhang B, Skrzypek E, Murray B, Latham V, Sullivan M. PhosphoSitePlus: a comprehensive resource for investigating the structure and function of experimentally determined post-translational modifications in man and mouse. Nucleic Acids Res. 2012; 40:D261–D270. [PubMed: 22135298]

Hubbell WL, Gross A, Langen R, Lietzow MA. Recent advances in site-directed spin labeling of proteins. Curr. Opin. Struct. Biol. 1998; 8:649–656. [PubMed: 9818271]

Isas JM, Langen R, Haigler HT, Hubbell WL. Structure and Dynamics of a Helical Hairpin and Loop Region in Annexin 12: A Site-Directed Spin Labeling Study†. Biochemistry (Mosc.). 2002; 41:1464–1473.

Itoh T, Erdmann KS, Roux A, Habermann B, Werner H, De Camilli P. Dynamin and the actin cytoskeleton cooperatively regulate plasma membrane invagination by BAR and F-BAR proteins. Dev. Cell. 2005; 9:791–804. [PubMed: 16326391]

Jao CC, Der-Sarkissian A, Chen J, Langen R. Structure of membrane-bound α-synuclein studied by site-directed spin labeling. Proc. Natl. Acad. Sci. U. S. A. 2004; 101:8331–8336. [PubMed: 15155902]

Jao CC, Hegde BG, Chen J, Haworth IS, Langen R. Structure of membrane-bound alpha-synuclein from site-directed spin labeling and computational refinement. Proc. Natl. Acad. Sci. U. S. A. 2008; 105:19666–19671. [PubMed: 19066219]

Jao CC, Hegde BG, Gallop JL, Hegde PB, McMahon HT, Haworth IS, Langen R. Roles of amphipathic helices and the bin/amphiphysin/rvs (BAR) domain of endophilin in membrane curvature generation. J. Biol. Chem. 2010; 285:20164–20170. [PubMed: 20418375]

Kukulski W, Schorb M, Kaksonen M, Briggs JAG. Plasma membrane reshaping during endocytosis is revealed by time-resolved electron tomography. Cell. 2012; 150:508–520. [PubMed: 22863005]

Lai C-L, Jao CC, Lyman E, Gallop JL, Peter BJ, McMahon HT, Langen R, Voth GA. Membrane binding and self-association of the epsin N-terminal homology domain. J. Mol. Biol. 2012; 423:800–817. [PubMed: 22922484]

Langen R, Oh KJ, Cascio D, Hubbell WL. Crystal structures of spin labeled T4 lysozyme mutants: implications for the interpretation of EPR spectra in terms of structure. Biochemistry (Mosc.). 2000; 39:8396–8405.

Lee E, Marcucci M, Daniell L, Pypaert M, Weisz OA, Ochoa G-C, Farsad K, Wenk MR, De Camilli P. Amphiphysin 2 (Bin1) and T-tubule biogenesis in muscle. Science. 2002; 297:1193–1196. [PubMed: 12183633]

Matta S, Van Kolen K, da Cunha R, van den Bogaart G, Mandemakers W, Miskiewicz K, De Bock P-J, Morais VA, Vilain S, Haddad D, et al. LRRK2 controls an EndoA phosphorylation cycle in synaptic endocytosis. Neuron. 2012; 75:1008–1021. [PubMed: 22998870]

Meinecke M, Boucrot E, Camdere G, Hon W-C, Mittal R, McMahon HT. Cooperative recruitment of dynamin and BIN/amphiphysin/Rvs (BAR) domain-containing proteins leads to GTP-dependent membrane scission. J. Biol. Chem. 2013; 288:6651–6661. [PubMed: 23297414]

Mim C, Cui H, Gawronski-Salerno JA, Frost A, Lyman E, Voth GA, Unger VM. Structural basis of membrane bending by the N-BAR protein endophilin. Cell. 2012; 149:137–145. [PubMed: 22464326]

Mizuno N, Jao CC, Langen R, Steven AC. Multiple Modes of Endophilin-mediated Conversion of Lipid Vesicles into Coated Tubes. J. Biol. Chem. 2010; 285:23351–23358. [PubMed: 20484046]

Moravcevic K, Alvarado D, Schmitz KR, Kenniston JA, Mendrola JM, Ferguson KM, Lemmon MA. Comparison of Saccharomyces cerevisiae F-BAR Domain Structures Reveals a Conserved Inositol Phosphate Binding Site. Struct. Lond. Engl. 2015 1993.

Nicot A-S, Toussaint A, Tosch V, Kretz C, Wallgren-Pettersson C, Iwarsson E, Kingston H, Garnier J-M, Biancalana V, Oldfors A, et al. Mutations in amphiphysin 2 (BIN1) disrupt interaction with dynamin 2 and cause autosomal recessive centronuclear myopathy. Nat. Genet. 2007; 39:1134–1139. [PubMed: 17676042]

Pang X, Fan J, Zhang Y, Zhang K, Gao B, Ma J, Li J, Deng Y, Zhou Q, Egelman EH, et al. A PH Domain in ACAP1 Possesses Key Features of the BAR Domain in Promoting Membrane Curvature. Dev. Cell. 2014

Peter BJ, Kent HM, Mills IG, Vallis Y, Butler PJG, Evans PR, McMahon HT. BAR domains as sensors of membrane curvature: the amphiphysin BAR structure. Science. 2004a; 303:495–499. [PubMed: 14645856]

Peter BJ, Kent HM, Mills IG, Vallis Y, Butler PJG, Evans PR, McMahon HT. BAR domains as sensors of membrane curvature: the amphiphysin BAR structure. Science. 2004b; 303:495–499. [PubMed: 14645856]

Pykäläinen A, Boczkowska M, Zhao H, Saarikangas J, Rebowski G, Jansen M, Hakanen J, Koskela EV, Peränen J, Vihinen H, et al. Pinkbar is an epithelial-specific BAR domain protein that generates planar membrane structures. Nat. Struct. Mol. Biol. 2011; 18:902–907. [PubMed: 21743456]

Rao Y, Haucke V. Membrane shaping by the Bin/amphiphysin/Rvs (BAR) domain protein superfamily. Cell. Mol. Life Sci. CMLS. 2011; 68:3983–3993.

Razzaq A, Robinson IM, McMahon HT, Skepper JN, Su Y, Zelhof AC, Jackson AP, Gay NJ, O'Kane CJ. Amphiphysin is necessary for organization of the excitation-contraction coupling machinery of muscles, but not for synaptic vesicle endocytosis in Drosophila. Genes Dev. 2001; 15:2967–2979. [PubMed: 11711432]

Saarikangas J, Zhao H, Pykäläinen A, Laurinmäki P, Mattila PK, Kinnunen PKJ, Butcher SJ, Lappalainen P. Molecular mechanisms of membrane deformation by I-BAR domain proteins. Curr. Biol. CB. 2009; 19:95–107.

Shah C, Hegde BG, Morén B, Behrmann E, Mielke T, Moenke G, Spahn CMT, Lundmark R, Daumke O, Langen R. Structural Insights into Membrane Interaction and Caveolar Targeting of Dynamin-like EHD2. Struct. Lond. Engl. 2014; 22:409–420. 1993.

Shimada A, Niwa H, Tsujita K, Suetsugu S, Nitta K, Hanawa-Suetsugu K, Akasaka R, Nishino Y, Toyama M, Chen L, et al. Curved EFC/F-BAR-domain dimers are joined end to end into a filament for membrane invagination in endocytosis. Cell. 2007; 129:761–772. [PubMed: 17512409]

Sorre B, Callan-Jones A, Manzi J, Goud B, Prost J, Bassereau P, Roux A. Nature of curvature coupling of amphiphysin with membranes depends on its bound density. Proc. Natl. Acad. Sci. U. S. A. 2012; 109:173–178. [PubMed: 22184226]

Takei K, Slepnev VI, Haucke V, De Camilli P. Functional partnership between amphiphysin and dynamin in clathrin-mediated endocytosis. Nat. Cell Biol. 1999; 1:33–39. [PubMed: 10559861]

Varkey J, Isas JM, Mizuno N, Jensen MB, Bhatia VK, Jao CC, Petrlova J, Voss JC, Stamou DG, Steven AC, et al. Membrane curvature induction and tubulation are common features of synucleins and apolipoproteins. J. Biol. Chem. 2010; 285:32486–32493. [PubMed: 20693280]

Varkey J, Mizuno N, Hegde BG, Cheng N, Steven AC, Langen R. α-Synuclein oligomers with broken helical conformation form lipoprotein nanoparticles. J. Biol. Chem. 2013; 288:17620–17630. [PubMed: 23609437]

Westphal CH, Chandra SS. Monomeric synucleins generate membrane curvature. J. Biol. Chem. 2013; 288:1829–1840. [PubMed: 23184946]

Wu T, Shi Z, Baumgart T. Mutations in BIN1 associated with centronuclear myopathy disrupt membrane remodeling by affecting protein density and oligomerization. PloS One. 2014; 9:e93060. [PubMed: 24755653]

Zhu C, Das SL, Baumgart T. Nonlinear sorting, curvature generation, and crowding of endophilin N-BAR on tubular membranes. Biophys. J. 2012; 102:1837–1845. [PubMed: 22768939]

Highlights

- Amphiphysin uses helical wedges and not its BAR domain for vesicle interaction.
- Amphiphysin uses oligomeric BAR domains to scaffold membrane tubes.
- Formation of oligomeric scaffold on tubes requires a threshold protein concentration.
- Membrane insertion pocket of BAR domain is site of numerous disease mutants.

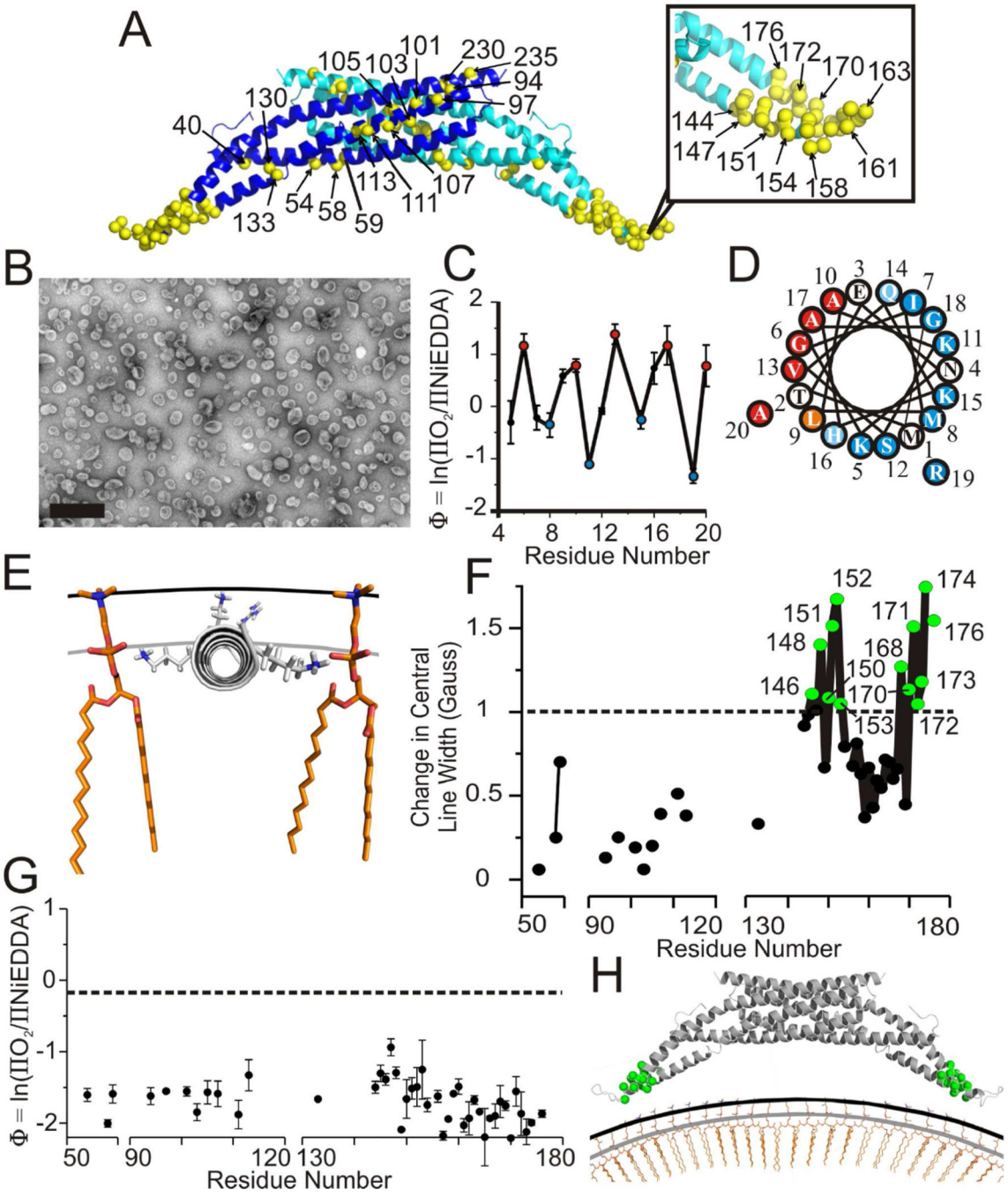

Figure 1. Amphiphysin binds vesicles with its N-terminus and not its BAR domain

(A) Crystal structure of homodimer drosophila amphiphysin (pdb 1URU) with individual subunits in blue and teal. Yellow α-carbons highlight residues in the BAR domain which were spin labeled (sequence numbers are provided for select sites). The N-terminal regions of amphiphysin are unresolved in the crystal structure and not shown.

(B) Negative stain electron microscopy image of amphiphysin bound to 100 nm vesicles composed of a 4:1 weight to weight ratio of 1-palmitoyl-2-oleoyl-*sn*-glycero-3-phospho-L serine and cholesterol. Scale bar = 500 nm.

(C) The depth parameter Φ for vesicle bound amphiphysin is plotted versus N-terminal spin labeling position.
(D) Helical wheel representation of the N-terminal region of amphiphysin. More deeply membrane inserted residues (red) and more solvent exposed residues (blue) are color coded as in (C).
(E) Model of amphiphysin's N-terminal helix bound to a vesicle membrane. The helix (gray) was manually placed according to immersion depths obtained from Φ values in Figure 1C and the calibration in Figure S1E (see text). Single phospholipids (orange) as well as the level of the lipid headgroups (black line) and phosphates (gray line) are displayed for reference.
(F) The change in central line width upon transitioning from solution to the vesicle bound form of amphiphysin is plotted versus spin labeled position. Positive changes indicate ordering upon vesicle binding. Sites with the largest changes (cutoff arbitrarily set at 1 Gauss) are highlighted (green).
(G) The depth parameter Φ for spin labeled sites in amphiphysin bound to 100 nm vesicles plotted versus labeled position. The ΠO_2 and ΠNiEDDA values used to calculate Φ are given in Figure S1D and Table S1. The Φ value obtained for a lipid moiety with a spin label at the position of the lipid headgroup (*see methods*) is displayed for reference (black dashed line).
(H) Model of amphiphysin's BAR domain bound to 100 nm vesicles. The N-termini are omitted for simplicity. Residues in the BAR domain that undergo line width changes greater than 1 Gauss upon binding vesicles are colored green as in Figure 1F. The location of the BAR domain relative to the membrane was estimated as described in the text. The level of the headgroups (black line) and lipid phosphates (gray line) are displayed for reference. Error bars represent SD, n = three independent experiments.

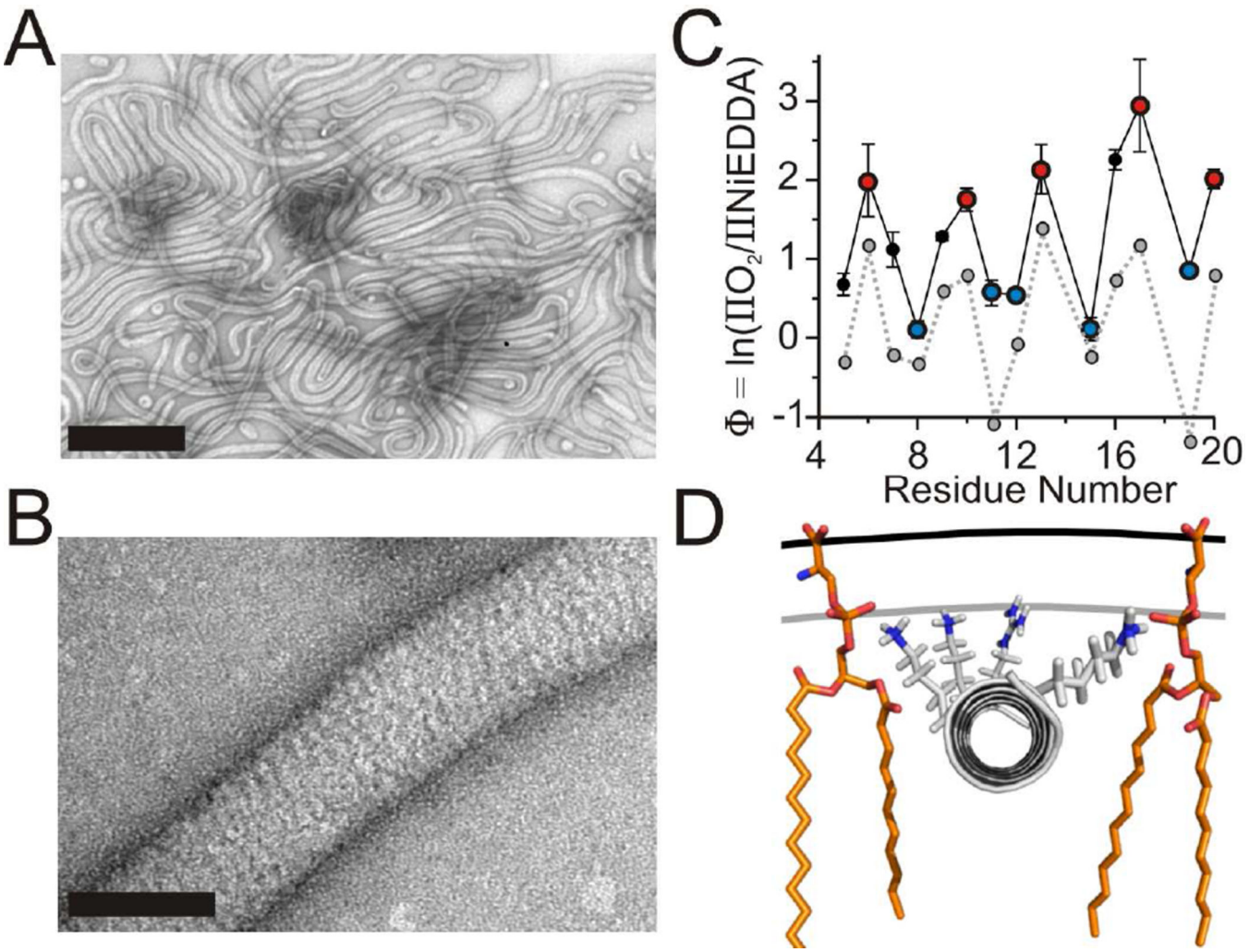

Figure 2. The N-terminus submerges into the acyl chain region on tubes

(A) Lipid tubes formed from large vesicles composed of a 2:1 weight to weight ratio of 1-palmitoyl-2-oleoyl-*sn*-glycero-3-[phospho-RAC-(1-glycerol)] and 1-palmitoyl-2-oleoyl-*sn*-glycero-3-phosphoethanolamine after incubation with amphiphysin at a 1:10 (protein:lipid) weight to weight ratio observed by negative stain electron microscopy. Scale bar = 500 nm.

(B) High magnification reveals a striated amphiphysin protein coat around a lipid tube. Scale bar = 50 nm.

(C) The depth parameter Φ as a function of residue number in the N-terminus on tubes. O_2 (red) and NiEDDA (blue) accessible residues are color coded similarly to the helical wheel in Figure 1D. Φ values obtained for vesicle bound amphiphysin (gray dashed line) from Figure 1C are plotted for comparison.

(D) Model of amphiphysin's N-terminus bound to tubes. The helix was manually placed according to the calibration (Figure S2D) and depth measurements (Figure 2C) as described in the text. Single lipids (orange) are displayed for reference. The plane of the headgroups (black line) and lipid phosphates (gray line) are displayed for reference. Error bars represent SD, n = three independent experiments.

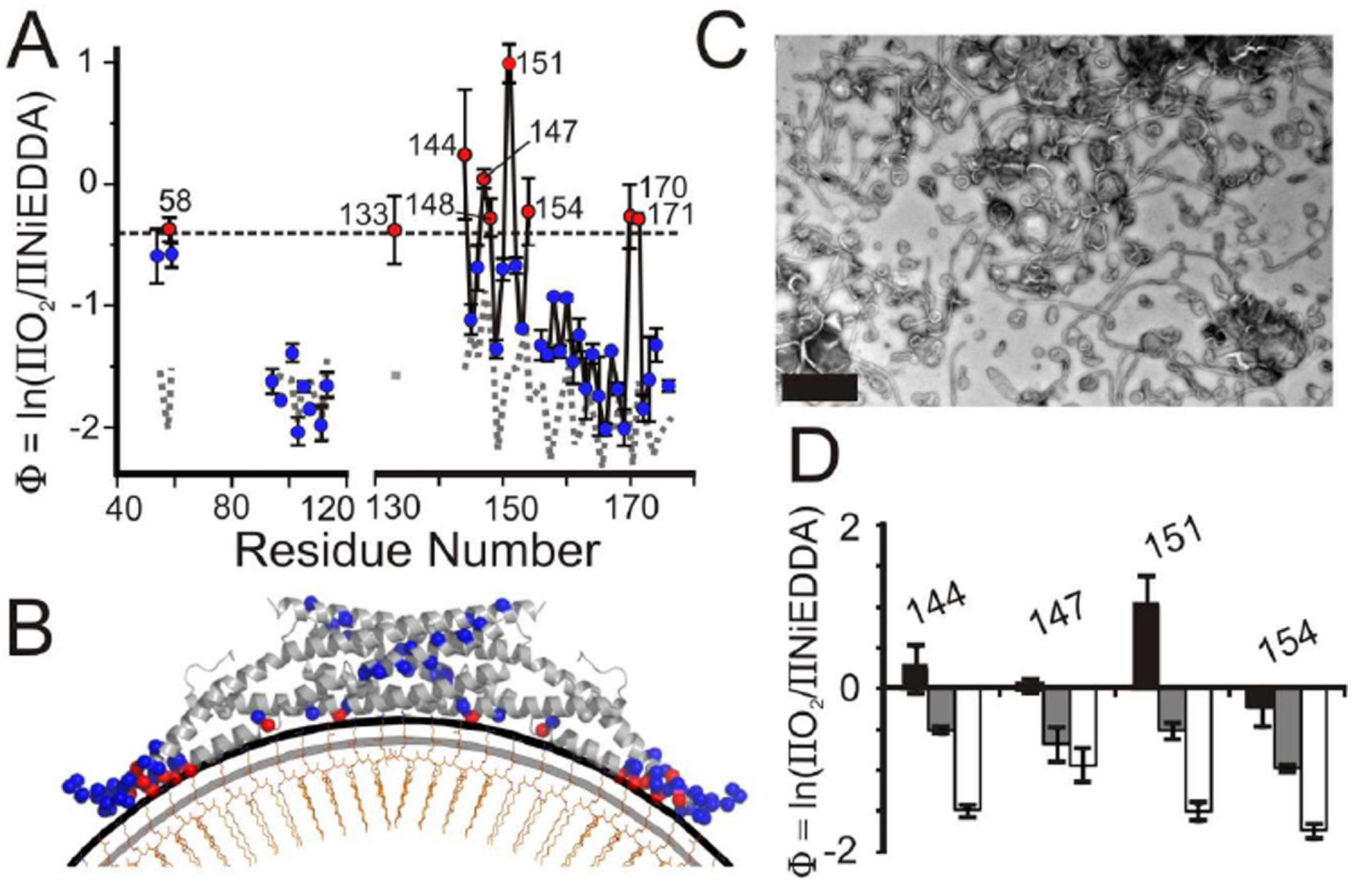

Figure 3. The BAR domain adheres its concave surface to the membrane on tubes

(A) The depth parameter, Φ, is plotted as function of the labeling position within the BAR domain of tube bound amphiphysin. The black dashed line corresponds to a headgroup location approximately 5 Å above the phosphate level (*see methods*; Figure S2D). Residues with Φ values equal to or greater than that of the dashed line are in red, while residues with smaller values are in blue. Φ values obtained for select residues of vesicle bound amphiphysin (gray dashed line) from Figure 1G are plotted for comparison.

(B) Model of amphiphysin's BAR domain bound to 100 nm vesicles with the N-terminal helices omitted for simplification. The level of the headgroups (black line) and lipid phosphates (gray line) on a lipid leaflet (orange) are schematically displayed for reference. α-carbons are color coded as in Figure 3A.

(C) Negative stain electron microscopy of a mixture of lipid tubes and small vesicles formed from large vesicles after incubation with amphiphysin at a 1:40 (protein:lipid weight ratio). Scale bar = 500 nm.

(D) Depth parameter (Φ) for select sites on the BAR domain when bound to tubes at various protein to lipid weight ratios; 1:10 (black) and 1:40 (gray). Φ values taken from Figure 1G for the same sites when bound to 100 nm vesicles (white) are also shown for reference (protein to lipid molar ratio of 1:10). Decreasing Φ values represent decreasing exposure of these sites to the membrane environment. Error bars represent SD, n = three independent experiments.

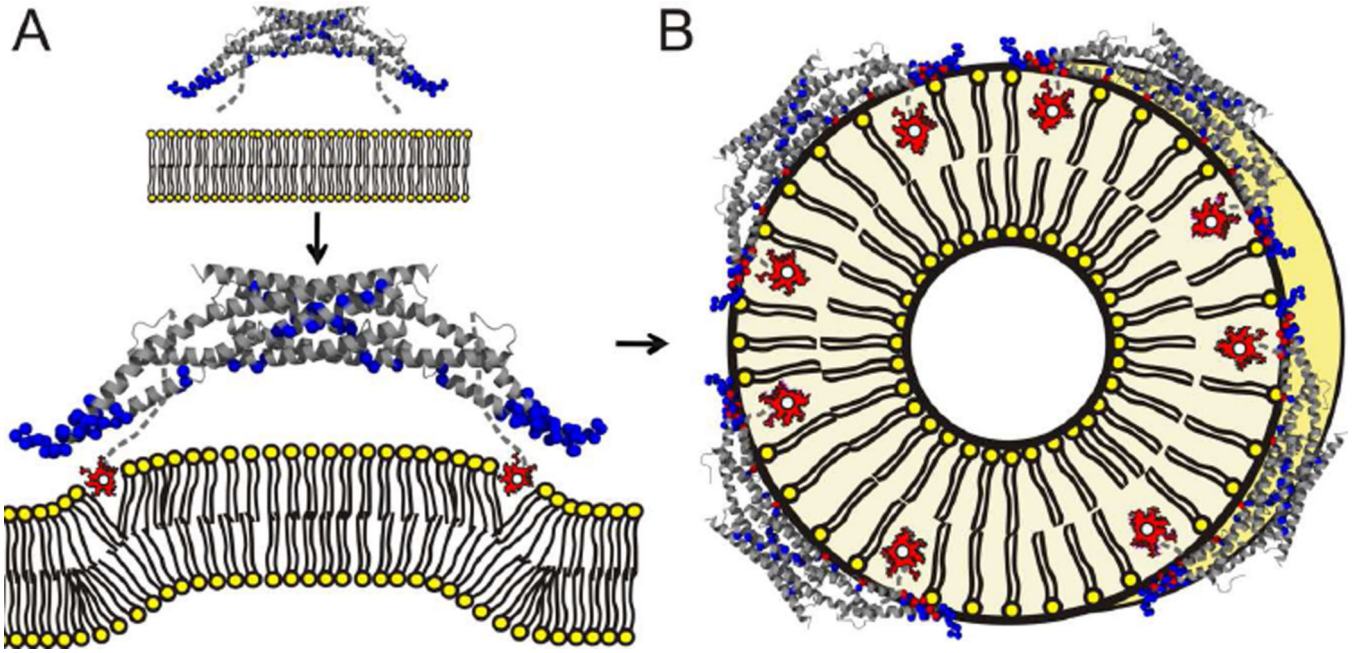

Figure 4. Model of how amphiphysin stabilizes different types of membrane curvature

(A) Upon contact with the membrane, the N-termini of amphiphysin are able to fold into amphipathic α-helices that embed (red is used for membrane exposed sites) into the membrane at the level of the lipid phosphates while the BAR domain remains distant (blue α-carbons represent solvent exposed spin sites). This state can either induce positive curvature by wedging apart lipid headgroups or sense already highly-curved membranes by stabilizing the existing packing defects in their outer leaflet. (B) At higher protein densities, amphiphysin oligomerizes, its BAR domain moves closer to the membrane and its helices insert more deeply into the membrane as tubes are formed.